

Heterogeneous & Homogeneous & Bio- & Nano-

CHEMCATCHEM

CATALYSIS

Accepted Article

Title: Green synthesis of rhodium nanoparticles, catalytically active in benzene hydrogenation and 1-hexene hydroformylation

Authors: Waleed Alsalahi, Włodzimierz Tylus, and Anna Trzeciak

This manuscript has been accepted after peer review and appears as an Accepted Article online prior to editing, proofing, and formal publication of the final Version of Record (VoR). This work is currently citable by using the Digital Object Identifier (DOI) given below. The VoR will be published online in Early View as soon as possible and may be different to this Accepted Article as a result of editing. Readers should obtain the VoR from the journal website shown below when it is published to ensure accuracy of information. The authors are responsible for the content of this Accepted Article.

To be cited as: *ChemCatChem* 10.1002/cctc.201701644

Link to VoR: <http://dx.doi.org/10.1002/cctc.201701644>

Green synthesis of rhodium nanoparticles, catalytically active in benzene hydrogenation and 1-hexene hydroformylation

W. Alsalahi^a, W. Tylus^b, A.M. Trzeciak^a

^a University of Wrocław, Faculty of Chemistry, 14 F. Joliot-Curie, 50-383 Wrocław, Poland

^b Department of Advanced Material Technologies, Faculty of Chemistry, Wrocław University of Science and Technology, Wybrzeże Wyspiańskiego 27, 50-370 Wrocław, Poland

Abstract

Rhodium nanoparticles (Rh NPs) were prepared according to a novel green methodology based on the reduction of (acetylacetonato)dicarbonylrhodium(I), Rh(acac)(CO)₂, in water at 80 °C. The nanoparticles, obtained without the addition of a reducing agent, were stabilized by polyvinylpyrrolidone (PVP) or polyvinyl alcohol (PVA) polymers and characterized by TEM (transmission electron microscopy), XPS (X-ray photoelectron spectroscopy), and XRD (X-ray powder diffraction) methods. The excellent catalytic activity of these Rh NPs was evidenced in the hydrogenation of benzene to cyclohexane. In the presence of PPh₃, Rh NPs formed a highly active system in the hydroformylation of 1-hexene. In this system, they acted as a source of soluble rhodium species.

Rh NPs were also synthesized in water using rhodium(II) acetate, Rh₂(OAc)₄, and rhodium(III) chloride, RhCl₃, as rhodium sources, and their catalytic activity was compared with that of the rhodium precursors.

Key words: rhodium; nanoparticles; hydrogenation, hydroformylation;

1. Introduction

Nanocatalysis is a rapidly growing field which involves the use of transition metal nanoparticles (NPs) as catalysts for a diversity of organic and inorganic reactions. Transition metal nanoparticles have been synthesized, according to the literature, using five general synthetic methods: (I) chemical reduction of transition metal salts, (II) ligand reduction and displacement from

organometallics, (III) thermal, photochemical, or sonochemical decomposition, (IV) electrochemical reduction, and (V) metal vapor synthesis. The most widely used method of NP preparation is the reduction of transition metal salts in the presence of stabilizing agents such as polymers or surfactants preventing NP agglomeration and crystal growth.^[1–8] Concerning polymers, polyvinylpyrrolidone (PVP) and polyvinyl alcohol (PVA) are commercially available, relatively cheap, nonpoisonous, water-soluble, and very effective stabilizing agents for NPs.^[9–10] While PVP was used very often for the stabilization of NPs, the application of PVA was only scarcely reported.^[10–12]

A wide range of reducing agents have been used in NP preparation, such as hydrogen or carbon monoxide, hydrides or salts (i.e. sodium borohydride or sodium citrate), or even oxidizable solvents, such as alcohols or glycols.^[4, 13–16]

Rhodium is one of the rarest and the most expensive transition metals. Nevertheless, this noble metal exhibits extraordinary and often unique catalytic properties in comparison with other noble metals, in particular in hydrogenation, hydroformylation, and oxidation reactions. Rh NPs are located at the boundary between homogeneous and heterogeneous catalysts.^[1, 16–17, 24] Their catalytic activity and selectivity depend on the shape, size, and composition of the stabilizing agents and ligands.^[4]

Hirai *et al.* reported the use of water-and-alcohol mixtures as reducing agents in the preparation of Rh, Pt, Pd, Os, or Ir NPs.^[18–24] Interestingly, Hirai observed that Rh NPs were not obtained in anhydrous methanol or in the absence of PVA. In contrast, RhCl_3 was reduced to Rh NPs after the addition of water to methanol. The presence of water during synthesis was essential for both metal reduction and stabilizing polymer dissolution.^[18] Rh NPs have also been prepared using ethylene glycol^[25] and vanadocene (Cp_2V) as reducing agents.^[26–27] All these NPs have been stabilized by extensively used organic polymers, PVP or PVA.

Interestingly, the size of Rh NPs depends on the amount of water used in the synthesis, the number of smaller NPs increases when the water content increases.^[28–29]

The hydrogenation of benzene to cyclohexane is one of the most important and intensively investigated reactions, in both laboratory and industrial synthetic chemistry. Cyclohexane is an important and essential chemical in the manufacturing of caprolactam, ϵ -caprolactone, polyamides, polyesters, nylon-6, and nylon-66. Millions of tons of cyclohexane are produced

annually by means of benzene hydrogenation,^[30–32] and several catalytic systems based on Rh NPs have been reported for this reaction.^[33–39]

There are a few papers dealing with the application of Rh NPs in the hydroformylation of olefins. In 1980, Smith used Rh NPs stabilized with a styrene/butadiene copolymer in the hydroformylation of 1-hexene at 100 °C and 42 bar of syngas and obtained 95% conversion to aldehydes with an n/iso ratio of 2.^[40] Liu *et al.* reported the hydroformylation of propylene catalyzed by a Rh/PVP colloid in a biphasic aqueous system.^[41] Bruss *et al.* obtained an n/iso ratio of 25 using 5 nm Rh NPs with the addition of Xantphos. They also observed Rh-carbonyl catalytically active species formed during the reaction.^[42] Rh NPs stabilized by poly(ethylene imine)/amide, employed in the hydroformylation of 1-hexene, gave 96% selectivity toward aldehydes and a 1.4 n/iso ratio. The formation of catalytically active complexes of the type $[\text{HRh}(\text{CO})_n\text{L}_m]$ was proposed in this reaction.^[43] Rh NPs stabilized with diphosphite ligands catalyzed the hydroformylation of styrene forming soluble active species.^[44] Han *et al.* reported the use of Rh NPs stabilized with (R)-BINAP ligands in the asymmetric hydroformylation of olefins, with high regioselectivity toward iso-aldehyde.^[45] Behr *et al.* described Rh NPs stabilized in a thermomorphic solvent as a catalyst for 1-dodecene hydroformylation with an n/iso ratio of 2.6, the n/iso ratio reaching 24 after the addition of a biphephos ligand.^[46] Rh NPs stabilized in an ionic liquid catalyzed the hydroformylation of 1-octene in a biphasic system, with 91% selectivity toward aldehydes, with a 1.4 n/iso ratio.^[47] Rh NPs immobilized in ZIF-8 exhibited high catalytic activity for the hydroformylation of alkenes and were easily separated and recycled five times without any remarkable loss in activity.^[48] High regioselectivity toward iso-aldehyde was reported for the hydroformylation of vinyl acetate with Rh NPs stabilized in TiO₂ nanotubes.^[49] The formation of soluble active species during hydroformylation was reported for Rh NPs stabilized by tetraoctylammonium bromide.^[50]

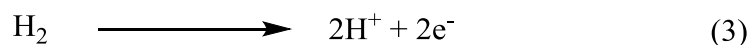
We have previously reported excellent chemoselectivity to aldehydes at a very high activity of the Rh catalyst in hydroformylation performed under water and solventless conditions.^[51–53]

In this paper, we present a new, simple and green, methodology of Rh NP synthesis by the reduction of rhodium species, Rh(acac)(CO)₂, Rh₂(OAc)₄, and RhCl₃, in a water medium, in the absence or in the presence of PVP or PVA polymers as stabilizing agents. The catalytic activity of the synthesized Rh NPs was successfully confirmed for the hydrogenation of benzene and the hydroformylation of 1-hexene in water.

2. Results and discussion

2.1. Synthesis of RhNPs

The unexpected formation of Rh NPs in reaction with water can be described by equations (1)–(4). Thus, water reacts with the carbonyl group according to the water gas shift scheme to produce carbon dioxide and hydrogen. Next, hydrogen acts as a reducing agent donating its electrons to Rh(I), which allows rhodium ions to be reduced to Rh NPs.



To the best of our knowledge, the efficient reduction of Rh(I) to Rh(0) by water has not been reported before. However, the important role of water in the reduction process was underlined by Hirai *et al.*^[26] They found that anhydrous alcohols were not efficient in the reduction of rhodium, whereas the presence of water enabled the successful synthesis of Rh NPs. This is in full agreement with our observations.

2.2. IR studies

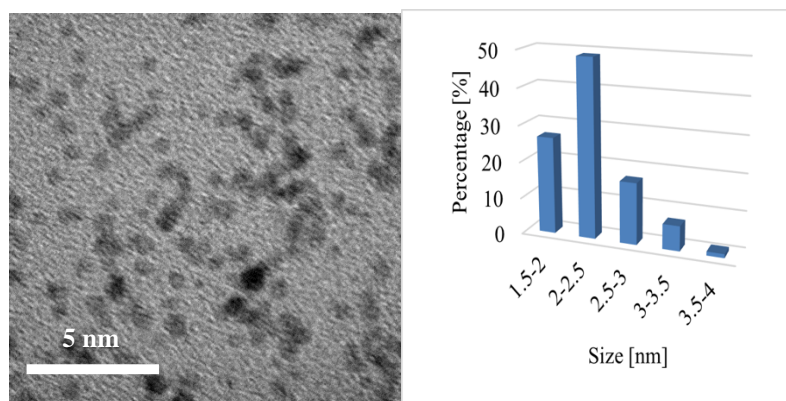
The IR spectrum of the product obtained after heating Rh(acac)(CO)₂ in a water medium without a polymer showed only a base line without any peaks characteristic for CO groups or for coordinated acac ligands (Fig. S1.). Consequently, the removal of those ligands from rhodium was evidenced. Similarly, the IR spectrum of the rhodium product obtained in the presence of PVP (Fig.S2-9) or PVA (Fig.S10-11) showed only peaks originating from the polymer.

2.3. TEM studies

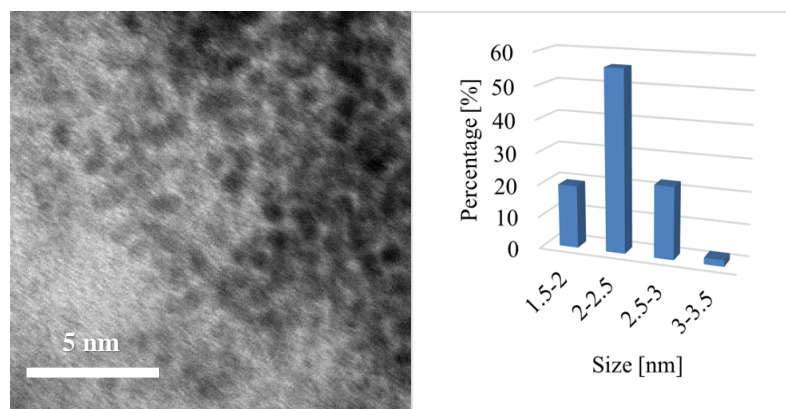
The morphology and nanoparticle size distribution were investigated by TEM analyses. Figures 1a–e show typical TEM images of freshly prepared Rh NPs synthesized by the reduction of Rh(acac)(CO)₂ in a water medium with different stabilizing agents or without them. They displayed uniform NP size distribution without any aggregation. The mean size of Rh NPs supported on polymers PVP-K30, PVP-K15, and PVA was 2–2.5 nm, while slightly bigger Rh NPs, 2.5–3 nm in diameter, were obtained in the absence of any stabilizing agent as shown in the histogram plot.

Similar TEM micrographs were also obtained for the product prepared from $\text{Rh}_2(\text{OAc})_4$ as the rhodium precursor (Fig. 1 f). However quite different results were observed by using $\text{RhCl}_3 \cdot 3\text{H}_2\text{O}$. In this case the TEM micrograph showed the significant aggregation of Rh NPs (Fig. 1 g).

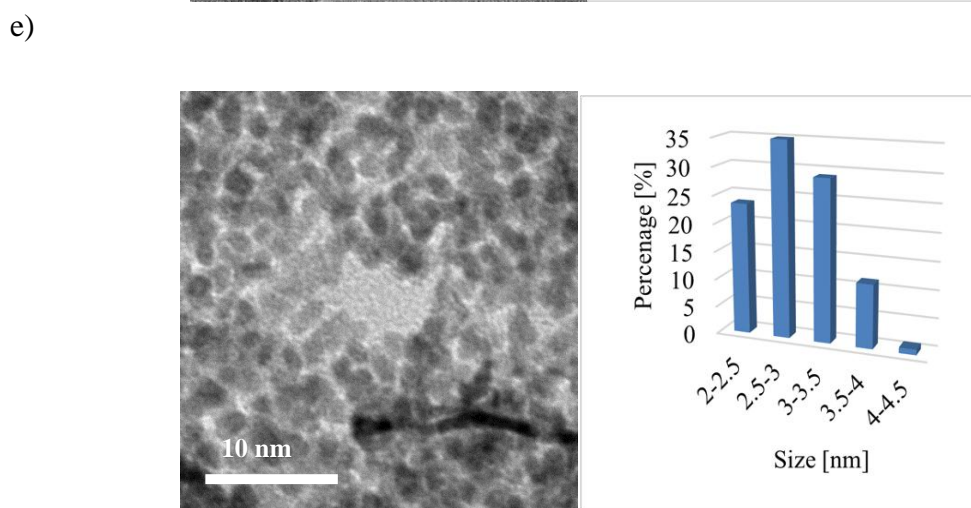
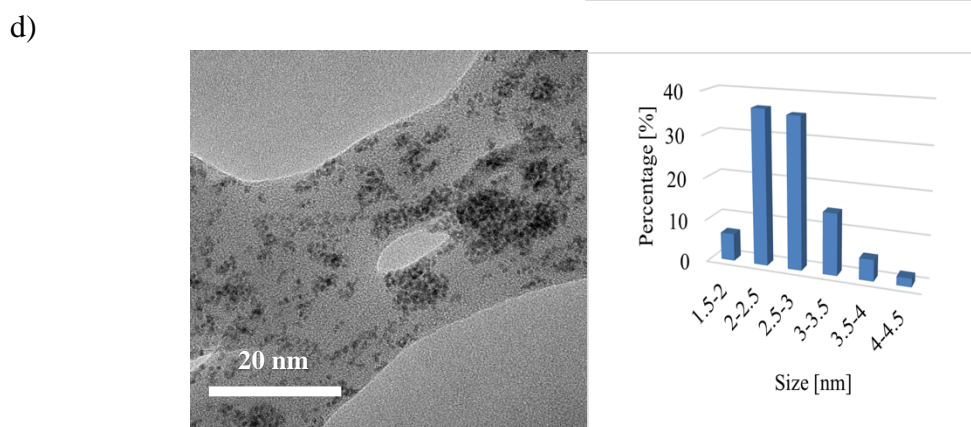
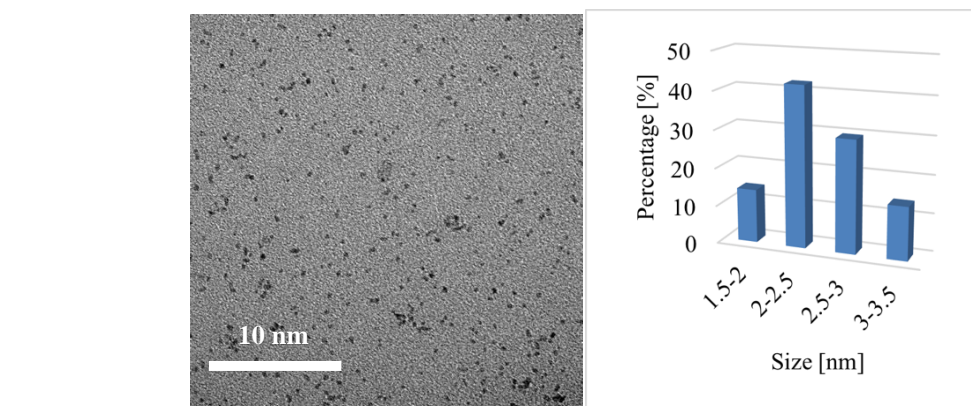
a)

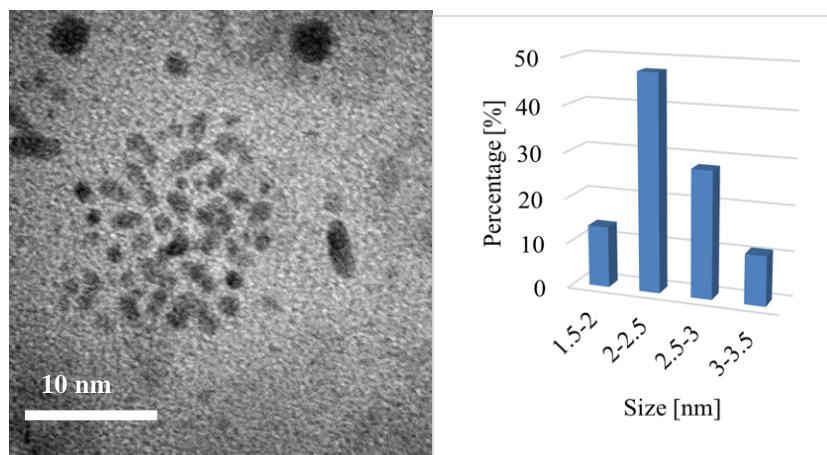


b)



c)





g)

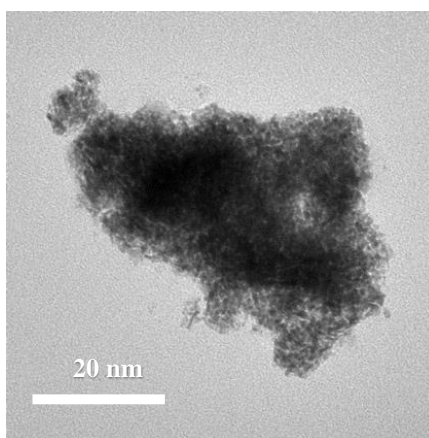


Fig. 1. Morphology and NP size distribution histograms of Rh NPs synthesized by the reduction of $\text{Rh}(\text{acac})(\text{CO})_2$ in a water medium at 80 °C: a. PVP-K30; b. PVP-K30 at room temperature; c. PVP-K15; d. PVA; e. without any stabilizing agent; f. $\text{Rh}_2(\text{OAc})_4$ as a precursor with PVP-K30; g. $\text{RhCl}_3 \cdot 3\text{H}_2\text{O}$ as a precursor with PVP-K30; More TEM images at low and high magnification and EDS spectra are in supplementary material (Fig. S18-24)

3.4. XRD studies

XRD measurements were performed for different time of XRD analysis with grinding and without grinding the sample (Fig. S12-17). Fig. 2. Shows the X-ray diffractograms of Rh NPs prepared by the reduction of $\text{Rh}(\text{acac})(\text{CO})_2$ in water showed a barely recognizable small peak at $2\theta = 41.1^\circ$ corresponding to the Rh(111) plane. No peaks were observed at 47.8° , 69.9° , and 84.5° corresponding to the (200), (220), and (311) planes, due to the small size of the nanoparticles (2 nm).^[56-57]

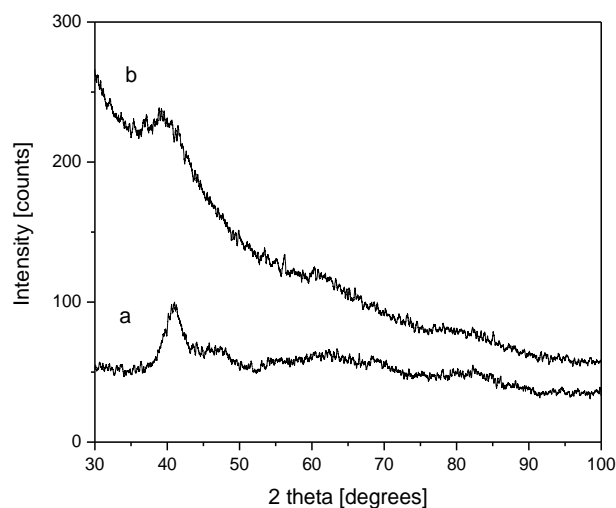


Fig. 2 X-ray diffraction pattern of rhodium nanoparticles synthesized by reducing $Rh(acac)(CO)_2$ as a precursor in a water medium: (a) without any stabilizing agent; (b) with PVP-K30.

3.5. XPS analysis

The Rh NPs have been analyzed by XPS to investigate the oxidation state of rhodium. The XPS spectrum showed two prominent bands at low BE values, 307 and 311.74 eV, typical for Rh(0), Rh($3d_{5/2}$) and Rh($3d_{3/2}$), respectively. Two additional bands at higher energy, 308.74 and 313.5 eV, are consistent with Rh_2O_3 and assigned to Rh(III) $3d_{5/2}$ and Rh(III) $3d_{3/2}$, respectively.^[58–59] Figure 3 presents the XPS spectrum of Rh/PVP as received (a) and after sputtering with argon ions (b). The spectrum shows an increase in the intensity of two bands of Rh(0) and a decrease in the intensity of Rh(III) bands after the surface was cleaned with argon.

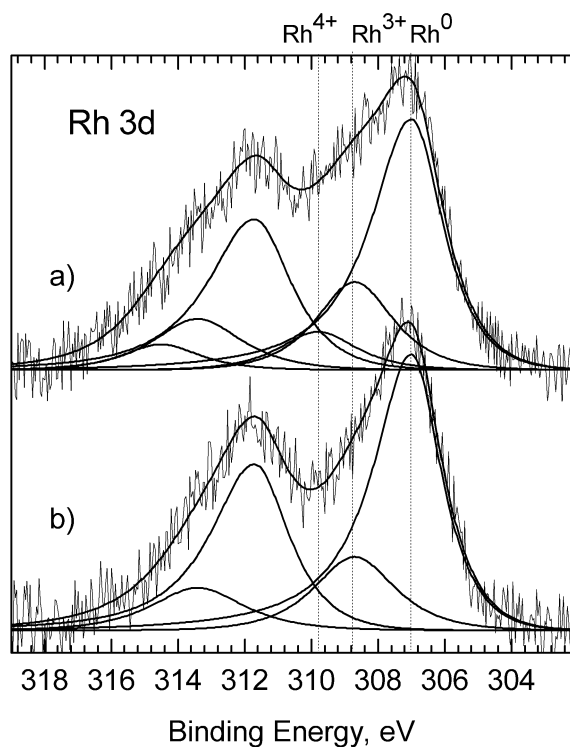


Fig.3 XPS spectra for Rh/PVP-K30; a) as received and b) after Ar⁺ cleaning (120s, 1.5 keV, 2 $\mu\text{A}/\text{cm}^2$)

The sample of Rh NPs prepared without a stabilizing agent contained more of Rh(0), 71.8%. After sputtering with argon ions, it demonstrated only bands assigned to Rh(0) (Fig. 4). Table 1 collects XPS data for the analyzed samples obtained from different rhodium precursors. As expected, when the same samples were analyzed after 2.3 months, the amount of oxidized Rh species increased, whereas the Rh(0) content decreased. Also, two additional bands were observed, at 309.75 and 314.49 eV, which can be attributed to RhO₂ and correspond to Rh(IV) 3d_{5/2} and Rh(IV) 3d_{3/2}, respectively, (Table S1 and Fig. S25-27).^[58–59] The rhodium oxides (Rh₂O₃ and RhO₂) could be formed during sample preparation and/or on the surface of rhodium nanoparticles upon exposure to air.^[60–61]

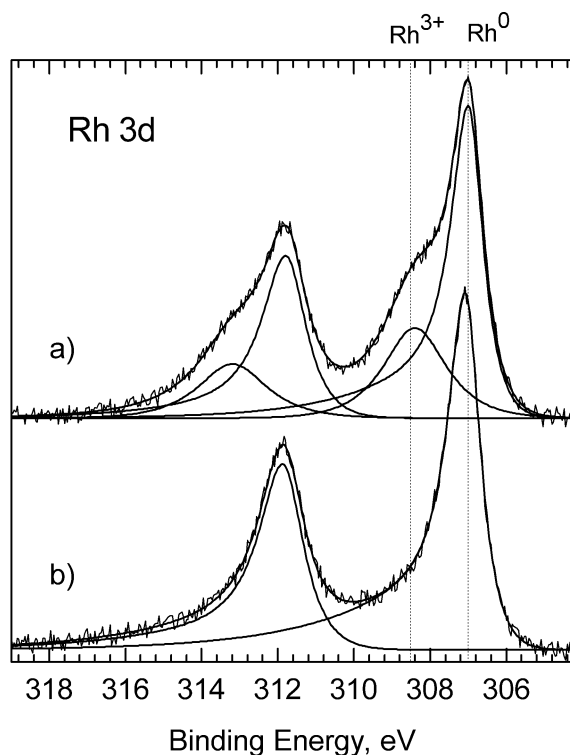


Fig.4 XPS spectra for Rh NPs without stabilizing agent (polymer); a) as received and b) after Ar^+ cleaning (120s, 1.5 keV, $2 \mu A/cm^2$)

Table 1. XPS data of rhodium samples prepared by reduction of different rhodium precursors in water.

Precursor	Stabilizing agent	Rh ⁰		Rh ₂ O ₃		Rh ⁺²	
		A%	B%	A%	B%	A%	B%
Rh(acac)(CO) ₂	PVP	17.8	79.3	82.2	20.7	0	0
	Without	71.8	100	28.2	0	0	0
Rh ₂ (OAc) ₄	PVP	0	87.3	0	0	100	12.7
	Without	0	54.9	0	0	100	45.1
RhCl ₃	PVP	0	43.5	0	0	100	56.5

A - as received; B – after sputtering with argon ion

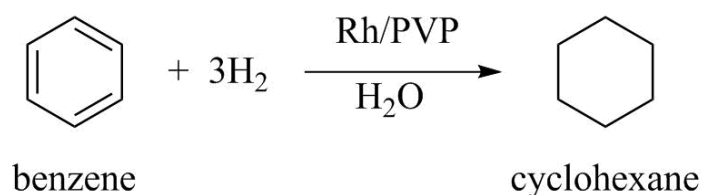
In Table 2 there are XPS data for different rhodium species collected in this work and found in the literature.

Table 2. Summary of XPS (Rh 3d_{5/2}) data for different rhodium species.

Sample		Binding energy 3d _{5/2} (eV)	Ref.
Rh ⁰	Rh metal	307	This work, [58, 59, 61] [62] [63]
		307.25	
		307.3	
Rh ⁺	Rh(acac)(CO) ₂	307.8	[64]
	Rh(CO) ₂ /γ-Al ₂ O ₃	307.9	
	Rh(CO) ₂ ⁺ / Al ₂ O ₃ -ZrO ₂	309.61	[65]
	Rh(CO)P ⁺ / Al ₂ O ₃ -ZrO ₂	309.75	
Rh ²⁺	Rh ₂ (OAc) ₄	309.02	This work,
Rh ³⁺	RhCl ₃	310	[66-68]
		310.3	
	Rh ₂ O ₃	308.7 308.5	This work, [58, 59] [63]
Rh ⁴⁺	RhO ₂	309.75	This work, [58, 59]

3.6. Hydrogenation of benzene

The catalytic activity of as-prepared Rh NPs was tested in the hydrogenation of benzene in water under relatively mild conditions: 80 °C and 20 bar of H₂. In all experiments, cyclohexane was formed as the only product.



Scheme 1. Hydrogenation of benzene

The obtained results illustrating the activity of different Rh NPs are summarized in Table 3. It was found that 19% of cyclohexane was formed when the reaction was carried out with Rh/PVP-K30 at 80 °C using 1.5 mL of benzene and 1.5 mL of water under 15 bar of H₂ (Table 3, entry 1). The yield of cyclohexane increased to 64% when the H₂ pressure increased to 20 bar (Table 3,

entry 2). An excellent conversion of benzene to cyclohexane (91%) was obtained when smaller amounts of benzene and water (1 mL of each) were used with the same catalyst (Table 3, entry 3). However, the activity of catalyst decreased by carrying out the same experiment after 2 months under the same condition, only 61 % of cyclohexane were obtained (Table 3. Entry 4) due to oxidation of catalyst. Increasing the concentration of catalyst, resulted in excellent conversion 95% (Table 3. Entry 5). Lower activity was noted when using Rh/PVP-K30 synthesized at room temperature as a catalyst. In that case, 64% of cyclohexane was formed (Table 3, entry 6). An excellent result, 100% yield of cyclohexane, was also obtained when Rh NPs immobilized on PVP-K15 was applied (Table 3, entry 7). However, when PVA was used as a support for Rh NPs, only 47% of cyclohexene was formed (Table 3, entry 8).

Good results were also obtained with Rh NPs used without any stabilizing agent. The yield of cyclohexane was 55 and 78% under solventless and under on-water conditions, respectively (Table 3, entries 9 and 10).

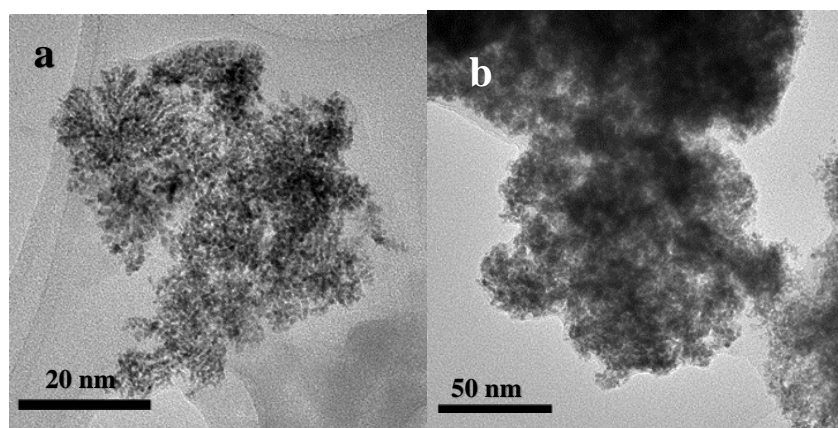
The next two catalysts, prepared from $\text{Rh}_2(\text{OAc})_4$ and $\text{RhCl}_3 \cdot 3\text{H}_2\text{O}$ and stabilized by PVP-K30, gave similarly good result, 60 and 88% of cyclohexane, respectively (Table 3, entries 11 and 12). In that case, it was interesting to compare whether pre-made NPs exhibit similar activity to those formed *in situ* from the same precursors. Interestingly, the application of $\text{RhCl}_3 \cdot 3\text{H}_2\text{O}$ without any pre-treatment resulted in a higher yield of cyclohexane, namely 100% (Table 3, entry 14). It also catalyzed hydrogenation under solventless conditions; however, the obtained conversions were lower (Table 3, entry 13). The *in situ* reduction of $\text{RhCl}_3 \cdot 3\text{H}_2\text{O}$ to Rh NPs was confirmed by the TEM analysis of the black suspension formed in the water phase during the hydrogenation of benzene. The TEM images demonstrated the presence of small Rh NPs with a symmetric size distribution, the mean size of NPs being located at 2.5–3 nm (Fig. 6). Bigger agglomerates were also observed. The organic phase did not contain any nanoparticles.

Table 3. Hydrogenation of benzene catalyzed by Rh NPs and Rh compounds.

Entry	Precursor for Rh NPs synthesis	Polymer	Cyclohexane%	TOF ^h , h ⁻¹
1	Rh(acac)(CO) ₂	PVP-K30	19 ^a	95
2			65 ^b	325

3			91	455
4			61 ^c	305
5			95 ^d	238
6			64 ^e	320
7		PVP-K15	65 (1 run)	216
7a			56 (2 run)	93
7b			35 (3 run)	58
7c			38 (4 run)	63
8		PVA	47 ^f	470
9		-	55 ^g	275
10		-	78	390
11	Rh ₂ (OAc) ₄	PVP-K30	60	300
12		PVP-K30	88	440
13	RhCl ₃ .3H ₂ O	-	45 ^g	225
14		-	100	500

Reaction conditions: benzene (1 mL), water (1 mL), [benzene]/[Rh] = 2000, *t* = 4 h, *T* = 80 °C, *P* = 20 bar; ^a *P* = 15 bar; ^{a and b} benzene (1.5 mL), water (1.5 mL); ^c catalyst was stored in air for 2 months before using; ^d [benzene]/[Rh] = 1000, ^e catalyst have been synthesized at r.t., ^f [benzene]/[Rh] = 4000; ^g reaction carried out under solventless conditions and ^h TOF = (mole of cyclohexane)/(mole of catalyst × reaction time)



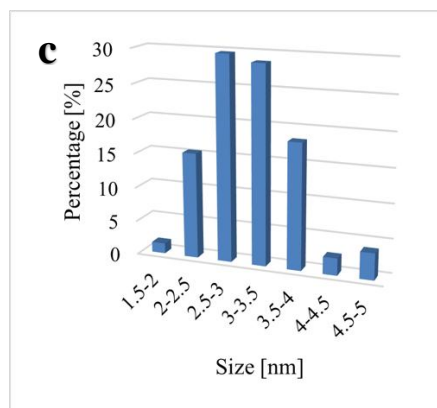
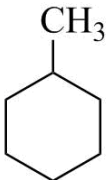
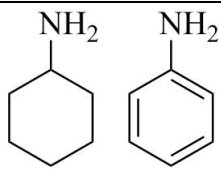


Fig 6. Morphology and nanoparticle size distributions of Rh NPs formed in situ during hydrogenation reaction of benzene in water medium catalyzed by $\text{RhCl}_3 \cdot \text{H}_2\text{O}$. a) non-aggregated nanoparticles, b) aggregated nanoparticles and c) histogram of Rh NPs size distribution.

Next, Rh NPs were tested in the hydrogenation of different arene derivatives in a water medium and under solventless conditions at 80 °C and under 20 bar hydrogen pressure. Rh NPs stabilized with PVP-K15 exhibited good activity in the hydrogenation of toluene, forming 70% of methylcyclohexane. In contrast, Rh/PVP-K30 achieved 30% yield (Table 4, entries 1 and 2, respectively). Unfortunately, Rh/PVP-K15 was inactive on hydrogenation of iodobenzene in water. Hydrogenation of nitrobenzene catalyzed by Rh/PVP-K30 in water and under solventless conditions resulted in its complete conversion to aniline (93.6% and 95.5%) and to cyclohexylamine (6.4 and 4.6%) (Table 4, entries 3 and 4).

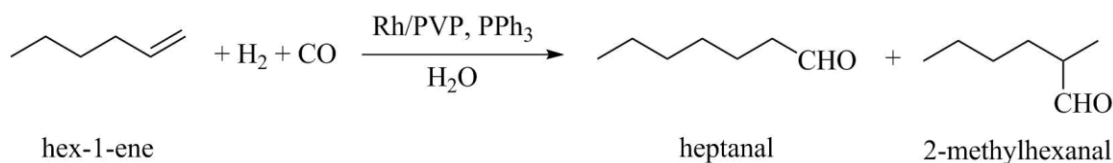
Table 4. Hydrogenation of different substrates catalyzed by Rh NPs.

Entry	Substrate	Catalyst	Solvent	Yield%	TOF ^a , h ⁻¹	Products
1		Rh/PVP-K15	Water	70	350	
2		Rh/PVP-K30		30	150	
3		Rh/PVP-K30	Water	6.4/93.6	468 ^b	
4			Solventless	4.5/95.5	477.5 ^b	

Reaction conditions: substrate (1 mL), water (1 mL), $[\text{substrate}]/[\text{Rh}] = 2000$, $t = 4$ h, $T = 80$ °C, $P = 20$ bar, ^a TOF = (mole of product)/(mole of catalyst x reaction time) and ^b TOF for aniline product.

3.7. Hydroformylation of 1-hexene

The hydroformylation of 1-hexene under on-water conditions was investigated by applying Rh NPs with a 13-fold excess of hydrophobic phosphine, PPh₃. In all experiments, aldehydes were the main products with a small amount of 2-hexene, the isomerization product (*ca.* 2–7%). Hydrogenation did not occur, and, consequently, hexane was not found. It was unexpected since Rh NPs are very active catalysts for the hydrogenation of alkenes and aromates. Clearly, CO efficiently inhibited hydrogenation.



Scheme 2. Hydroformylation of 1-hexene

First, we studied the reaction using Rh/PVP-K30 alone; however, no conversion of 1-hexene was observed (Table 5, entry 1). However, already a 6-fold excess of PPh₃ was sufficient to achieve 79% conversion to corresponding aldehydes with an *n*/*iso* ratio of 3.2 (Table 5, entry 2). An increase in the amount of PPh₃ to a 13-fold excess resulted in a high conversion of 1-hexene (96%) with 90% selectivity to aldehydes (75% of 1-heptanal and 15% of 2-methyl-hexanal) (Table 5, entry 3). Thus, an excess of PPh₃ caused a remarkable increase in the conversion of 1-hexene and an increase in the *n*/*iso* ratio from 3.2 to 5. This is in agreement with the literature data: that a high yield of linear aldehydes increases with higher phosphine excess.^[69] The same excellent results were obtained when other Rh NPs synthesized from Rh(acac)(CO)₂ and stabilized by PVP-K15 and PVA were applied (Table 5, entries 5 and 6). Rhodium nanoparticles used without a stabilizing agent gave 83% and 94% conversion on water and under solventless conditions, respectively (Table 5, entries 7 and 8). Very good results were obtained when applying Rh/PVP-K30 synthesized from Rh₂(OAc)₄, with the *n*/*iso* ratio of 5.1 at 88% conversion (Table 5, entry 9). In contrast, the catalyst obtained by the reduction of the RhCl₃·3H₂O complex, Rh/PVP-K30, was not active in the hydroformylation of 1-hexene on water, probably due to the aggregation of nanoparticles (Table 5, entry 10).

Table 5. Hydroformylation of 1-hexene catalyzed by rhodium nanoparticles.

Entry	Precursor for Rh NPs synthesis	Polymer	[PPh ₃]/[Rh]	Conv. %	2-hexene %	Aldehydes %	n/iso	TOF ^e , h ⁻¹
1	Rh(acac)(CO) ₂	PVP-K30	0	0				0
2			6	79		79	3.2	197.5
3			13	96	6	90	5	225
4 ^a			13	96	7	89	5.4	320
5		PVP-K15	13	88	5	83	5	220
6 ^b		PVA	13	96	4	92	3.4	608
7		-	13	83	9	74	3.1	207.5
8 ^c		-	13	94	3	91	3.9	235
9 ^d	Rh ₂ (OAc) ₄	PVP-K30	19.6	84	5	79	5.1	315
10	RhCl ₃ ·3H ₂ O		13	0				0

Reaction conditions: 1-hexene (1.5 mL), water (1.5 mL), [1-hexene]/[Rh] = 1000, T = 80 °C, P = 10 bar (H₂/CO=1), t = 4 h, ^{a and b} t = 3h, ^c catalyst prepared at room temperature; ^{b and d} [sub]/[Rh] = 1900 and 1500, respectively; ^e reaction carried out under solventless conditions and ^e TOF= (mole of aldehydes)/(mole of catalyst x reaction time).

3.8. Studies of catalysts composition after catalytic reaction

The Rh/PVP catalysts separated after catalytic reactions were analyzed by XPS and TEM methods to determine their structure. The catalyst Rh/PVP-K30 examined after benzene hydrogenation contained 87% of Rh(0) and 13% of Rh(III) (Fig. 7a). The Rh/PVP-K30 catalyst isolated from the hydroformylation reaction mixture contained 92.5% of Rh(0) and 7.5% of Rh(III) (Fig. 7b).

The Rh/PVP-K15 catalyst recovered after four subsequent runs of benzene hydrogenation was also analyzed. According to TEM micrographs the sample is composed of organic compounds and small Rh(0) nanocrystallites (Figure 8). The Rh(0) nanoparticles are approximately 2 nm large. They are arranged in branched chain-like species with an overall length about 20-30 nm.

These experiments confirmed good stability of the studied catalysts under catalytic reaction conditions.

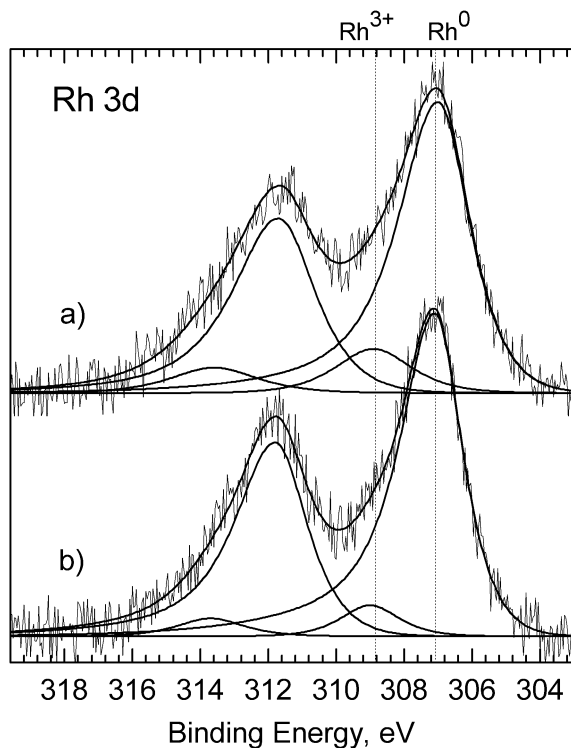


Fig.7 XPS spectra for a) Rh/PVP-K30 after benzene hydrogenation b) Rh/PVP-K30 after 1-hexene hydroformylation

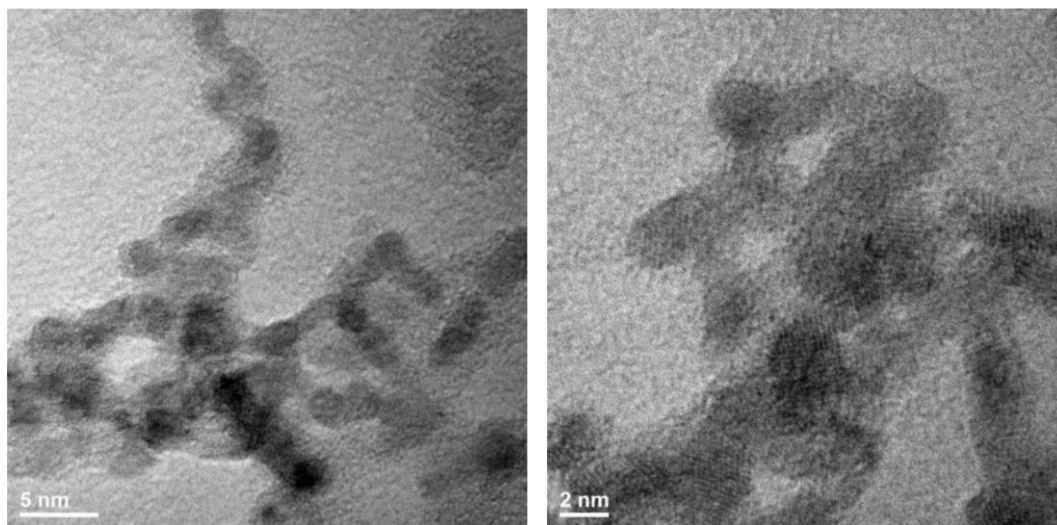


Fig 8. TEM micrographs of the sample of Rh/PVP-K15 after benzene hydrogenation.

4. Conclusions

Rhodium nanoparticles were prepared from Rh(acac)(CO)₂ suspended in water, in the presence of a water-soluble polymer (such as polyvinylpyrrolidone, PVP, or polyvinyl alcohol, PVA) as the

stabilizing agent at room temperature and at 80 °C. This new methodology is especially attractive, operationally simple and green, as it is highly effective without any addition of a reducing agent or an organic solvent. Rhodium nanoparticles were obtained with water as the only reducing agent.

The same method was also applied to get Rh NPs from other rhodium substrates, $\text{Rh}_2(\text{OAc})_4$ and RhCl_3 . In the samples isolated after heating in water, Rh(0) was not found by XPS; however, TEM confirmed the presence of Rh NPs. The sputtering of the surface with argon resulted in the appearance of XPS bands characteristic of Rh(0).

The diameter of Rh NPs obtained by water reduction was *ca.* 2 nm, and they were uniformly distributed in the polymer. Only in the case of RhCl_3 was the agglomeration of nanoparticles observed.

Rh/PVP catalysts display excellent catalytic performance in the hydrogenation reaction of benzene to cyclohexane under biphasic conditions (benzene/water). Similarly, high activity was also noted for Rh NPs prepared without a stabilizing agent.

The same catalysts showed very high catalytic activity and high regioselectivity to heptanal (linear aldehyde) in the hydroformylation of 1-hexene under on-water conditions. In those reactions, Rh NPs acted as a source of soluble, catalytically active species.

5. Experimental

5.1. Materials

The rhodium complexes $\text{Rh}(\text{acac})(\text{CO})_2$ and $\text{Rh}_2(\text{OAc})_4$ was prepared according to the literature.^[54, 55] $\text{RhCl}_3 \cdot 3\text{H}_2\text{O}$ was purchased from Riedel-de Haën, polyvinylpyrrolidones (K15(Mw ~ 10,000) and K30(Mw ~ 40,000)) were purchased from Fluka, polyvinyl alcohol was purchased from Sigma-Aldrich; triphenylphosphine (PPh_3) was purchased from Avocado; 1-hexene was purchased from Merck; benzene was purchased from Sigma-Aldrich; hydrogen (H_2 , 99.999%) and carbon monoxide (CO , 99.97%) were procured from Air Products. All chemicals were used without any additional purification. Distilled water was used as the reaction medium.

5.2. Synthesis Rh NPs in water

A solution of polyvinylpyrrolidone (K-30, Mw ~ 40 000; or K-15, Mw ~ 10 000) or polyvinyl alcohol (0.48 g) dissolved in water (10 mL) was added to a suspension of $\text{Rh}(\text{acac})(\text{CO})_2$ (2.4×10^{-4} mol) in water (10 mL). The mixture was stirred for 2 h at 80 °C and for 24 h at room

temperature and filtered. The resulting solution was evaporated to dryness using a rotary vacuum evaporator yielding a film of polymer-stabilized Rh NPs (Table 6, entries 1–4). Table 6 shows the colors of the products and the content of rhodium determined by ICP. The same procedure was used to obtain rhodium nanoparticles from other rhodium species and without a stabilizing agent (Table 6, entry 5).

Attempts to obtain Rh NPs by the same method, namely heating a rhodium compound in a water medium, were also performed using $\text{Rh}_2(\text{OAc})_4$ and $\text{RhCl}_3 \cdot 3\text{H}_2\text{O}$ as the rhodium sources (Table 6, entries 6 and 7).

The product obtained from $\text{Rh}(\text{acac})(\text{CO})_2$ in water at room temperature was yellow, whereas all the other products, prepared at 80 °C, were black. However, the use of $\text{Rh}_2(\text{OAc})_4$ or $\text{RhCl}_3 \cdot 3\text{H}_2\text{O}$ as rhodium precursors afforded dark blue or dark brown products, respectively. The content of rhodium in the obtained materials was determined by means of ICP. The rhodium content was the lowest, 1.9 wt.% Rh, when the reaction was carried out at room temperature, while it increased to 3.7% when the synthesis was performed at 80 °C, using PVP-K30 as the stabilizing agent (Table 6, entries 1 and 2). The amount of rhodium in the final material also varied with the change of the stabilizing polymer and the rhodium precursor (Table 6).

Table 6. Synthesis of rhodium nanoparticles in a water medium.

Entry	Precursor	Polymer	T, °C	t, h	Color	Rh% ^a	Particle size[nm] ^b
1	$\text{Rh}(\text{acac})(\text{CO})_2$	PVP-K30	Rt.	24	Yellow	1.9	2-2.5
2			80	2	Black	3.7	2-2.5
3		PVP-K15	80	2		4.4	2-2.5
4		PVA	80	2		3.2	2-2.5
5		-	80	2		2.5-3	
6	$\text{Rh}_2(\text{OAc})_4$	PVP-K30	80	20	blue	7.7	2-2.5
7	$\text{RhCl}_3 \cdot 3\text{H}_2\text{O}$		80	2	brown	3.9	aggregation

^a Rhodium content determined by ICP; ^b Average size of rhodium particles determined by counting the size of approximately 200–300 rhodium nanoparticles from several TEM images.

5.3. Sample preparation for ICP measurements

A 0.02 g sample of Rh/PVP was placed in a 25 mL volumetric flask, and the flask was filled to 25 ml with distilled water and then stirred until the complete dissolution of solids.

5.4. Hydrogenation of benzene

Hydrogenation reactions were carried out in a 50 mL stainless steel autoclave equipped with a manometer, a thermostat, a magnetic stirrer, and a gas inlet/outlet system. The catalyst (5.5×10^{-6} mol) was introduced in the autoclave under nitrogen atmosphere. 1 mL of benzene (0.011 mol) and 1 mL of water were placed in the autoclave. The autoclave was closed, filled with hydrogen (5 bar) three times, and then pressurized with hydrogen to 20 bar and heated to 80 °C for 4 h. After the reaction was finished, the autoclave was cooled down to room temperature and depressurized. The organic products were separated by a vacuum transfer procedure and analyzed by means GC and GC-MS.

5.5. Hydroformylation of 1-hexene

Hydroformylation experiments were carried out in a 50 mL stainless steel autoclave equipped with a manometer, a thermostat, a magnetic stirrer, and a gas inlet/outlet system. The catalyst (1.2×10^{-5} mol of Rh) and PPh_3 (1.56×10^{-4} mol) were introduced in the reactor under nitrogen atmosphere, and 1.5 mL (0.012 mol) of 1-hexene and 1.5 mL of water were introduced. The autoclave was closed, flushed with hydrogen (5 bar) three times, and then pressurized with the synthesis gas (H_2 : CO = 1: 1) to 10 bar and heated to 80 °C for 4 h. Afterwards, the autoclave was cooled down to the ambient temperature and depressurized. The organic products were separated by a vacuum transfer procedure and analyzed by means GC and GC-MS.

Acknowledgements

XPS studies were financed by a statutory activity subsidy from the Polish Ministry of Science and Higher Education for the Faculty of Chemistry of Wrocław University of Technology.

Authors thank to prof. L. Kępiński and to dr W. Gil for performance of TEM measurements and to dr A. Gniewek for technical assistance.

References

- [1] S. J. Kraft, G. Zhang, D. Childers, F. Dogan, J. T. Miller, S.T. Nguyen, and A. S. Hock; *Organometallics* **2014**, *33*, 2517–2522.
- [2] A. Roucoux, J. Schulz, and H. Patin., *Chem. Rev.* **2002**, *102*, 3757–3778.
- [3] J. D. Aiken, R. G. Finke, *J. M. Catal. A: Chem.* **1999**, *145*, 1–44.

- [4] C. J. Jia and F. Schuth, *Phys. Chem. Chem. Phys.* **2011**, *13*, 2457–2487.
- [5] C. Amiens, B. Chaudret, D. Ciuculescu-Pradines, V. Colliere, K. Fajerweg, P. Fau, M. Kahn, A. Maisonnat, K. Soulantica and K. Philippot, *New J. Chem.* **2013**, *37*, 3374–3401.
- [6] R. Narayanan and M. A. El-Sayed, *J. Phys. Chem. B* **2005**, *109*, 12663–12676.
- [7] C. Burda, X. Chen, R. Narayanan, and M. A. El-Sayed, *Chem. Rev.* **2005**, *105*, 1025–1102.
- [8] *Metal nanoparticles for catalysis: advances and applications*, ed. F. Tao and J. J. Spivey; Royal Society of Chemistry (Great Britain), **2014**.
- [9] H. Thiele, H.S. von Lavern, *J. Colloid Sci.* **1965**, *20*, 679–694.
- [10] Y. Zhao, J. A. Baeza, N. K. Rao, L. Calvo, M. A. Gilarranz, Y.D. Li and L. Lefferts, *J. Catal.* **2014**, *318*, 162–169.
- [11] L. M. Rossi, L. L. R. Vono, M. A. S. Garcia, T. L. T. Faria and J. A. Lopez-Sanchez, *Top. Catal.* **2013**, *56*, 1228–1238.
- [12] Z. H. Mbhele, M. G. Salemane, C. G. C. E. van Sittert, J. M. Nedeljkovic, V. Djokovic, and A. S. Luyt, *Chem. Mater.* **2003**, *15*, 5019–5024.
- [13] L. N. Lewis, *Chem. Rev.* **1993**, *93*, 2693–2730.
- [14] B. L. Cushing, V. L. Kolesnichenko, and C. J. O'Connor, *Chem. Rev.* **2004**, *104*, 3893–3946.
- [15] L. D. Pachon and G. Rothenberg, *Appl. Organometal. Chem.* **2008**, *22*, 288–299.
- [16] M. Guerrero, N.T. T. Chau, S. Noël, A. D. Nowicki, F. Hapiot, A. Roucoux, E. Monflier, and K. Philippot., *Curr. Org. Chem.* **2013**, *17*, 364–399.
- [17] L. Barthe, A. Denicourt-Nowicki, A. Roucoux, K. Philippot, B. Chaudret and M. Hemati, *Catal. Commun.* **2009**, *10*, 1235–1239.
- [18] H. Hirai, Y. Nakao, N. Toshima and K. Adachi, *Chem. Lett.* **1976**, *5*, 905–910.
- [19] H. Hirai, *J. Macromol. Sci. Chem. A* **1979**, *13*, 633–649.
- [20] Q. Wang, H. Liu, M. Han, X. Li and D. Jiang, *J. Mol. Catal. A: Chem.* **1997**, *118*, 145–151.
- [21] A. Borsla, A. M. Wilhelm and H. Delmas, *Catal. Today* **2001**, *66*, 389–395.
- [22] H. Ma, H. Chen, Q. Zhang and X. Li, *J. Mol. Catal. A: Chem.* **2003**, *196*, 131–135.
- [23] T. Ashida, K. Miura, T. Nomoto, S. Yagi, H. Sumida, G. Kutluk, K. Soda, H. Namatame and M. Taniguchi, *Surf. Sci.* **2007**, *601*, 3898–3901.

- [24] A. Gniewek and A. M. Trzeciak., *Top Catal.* **2013**, *56*,1239–1245.
- [25] S. García, J. J. Buckley, R. L. Brutchey and S. M. Humphrey, *Inorg. Chim. Acta* **2014**, *422*, 65–69.
- [26] J. L. Pellegatta, C. Blandy, V. Colliere, R. Choukroun, B. Chaudret, P. Cheng and K. Philippot, *J. Mol. Catal. A: Chem.* **2002**, *178*, 55–61.
- [27] M. Kopaczynska, J. H. Fuhrhop, A. M. Trzeciak, Jozef J. Ziolkowski and R. Choukroun, *New J. Chem.* **2008**, *32*, 1509–1512.
- [28] C. Burda, X. Chen, R. Narayanan, and M. A. El-Sayed, *Chem. Rev.* **2005**, *105*, 1025–1102.
- [29] C.-J. Jia and F. Schuth, *Phys. Chem. Chem. Phys.* **2011**, *13*, 2457–2487.
- [30] G. S. Fonseca, A. P. Umpierre, P. F. P. Fichtner, S. R. Teixeira, J. Dupont, *Chem. Eur. J.* **2003**, *9*, 3263–3269.
- [31] H. Liu, R. Fang, Z. Li and Y. Li, *Chem. Eng. Sci.* **2015**, *122*, 350–359.
- [32] L. Zhu, H. Sun, H. Fu, J. Zheng, N. Zhang, Y. Li and B. H. Chen, *Appl. Catal. A: Gen.* **2015**, *499*, 124–132.
- [33] J. Schulz, A. Roucoux, and H. Patin, *Chem. Eur. J.* **2000**, *6*, 618–624.
- [34] X. Mu, J. Meng, Z. Li, and Y. Kou, *J. Am. Chem. Soc.* **2005**, *127*, 9694–9695.
- [35] I. S. Park, M. S. Kwon, N. Kim, J. S. Lee, K. Y. Kang and J. Park, *Chem. Commun.* **2005**, 5667–5669.
- [36] K. H. Park, K. Jang, H. J. Kim, and S. Uk Son, *Angew. Chem. Int. Ed.* **2007**, *46*, 1152–1155.
- [37] C. Zhao, H. Wang, N. Yana, C. Xiao, X. Mua, P. J. Dysonb and Y. Kou, *J. Catal.* **2007**, *250*, 33–40.
- [38] X. Yang, N. Yan, Z. Fei, R. M. C. Quesada, G. Laurency, L. K. Minsker, Yuan Kou, Y. Li, and P. J. Dyson, *Inorg. Chem.* **2008**, *47*, 7444–7446.
- [39] M. J. Jacinto, P. K. Kiyohara, S. H. Masunaga, R. F. Jardim and L. M. Rossi, *Appl. Catal. A Gen.* **2008**, *338*, 52–57.
- [40] US 4252678 (**1981**), Xerox Corporation, invs.: T. W. Smith.
- [41] M. Han, H. Liu, *Macromol. Symp.* **1996**, *105*, 179–183.
- [42] A. J. Bruss, M. A. Gelesky, G. Machado, J. Dupont, *J. Mol. Catal. A: Chem.* **2006**, *252*, 212–218.

- [43] L. Tuchbreiter and S. Mecking, *Macromol. Chem. Phys.* **2007**, *208*, 1688–1693.
- [44] M. R. Axet, S. Castillon, C. Claver, K. Philippot, P. Lecante, and B. Chaudret, *Eur. J. Inorg. Chem.* **2008**, 3460–3466.
- [45] D. Han, X. Li, H. Zhang, Z. Liu, G. Hu and C. Li, *J. M. Catal. A Chem.* **2008**, *283*, 15–22.
- [46] A. Behr, Y. Brunsch and A. Lux, *Tetrahedron Lett.* **2012**, *53*, 2680–2683.
- [47] Z. Yan, W. Yanhua, X. Yicheng, S. Ying, Z. Jiaqi, J. Jingyang and J. Zilin, *Chin. J. Catal.* **2012**, *33*, 402–406.
- [48] C. Hou, G. Zhao, Y. Ji, Z. Niu, D. Wang, and Y. Li, *Nano Res.* **2014**, *7(9)*, 1364–1369.
- [49] Y. Shi, X. Hu, B. Zhu, S. Wang, S. Zhang and W. Huang, *RSC Adv.* **2014**, *4*, 62215–62222.
- [50] M. A. S. Garcia, K. C. B. Oliveira, J. C. S. Costa, P. Corio, E. V. Gusevskaya, E. N. dos Santos, and L. M. Rossi, *ChemCatChem* **2015**, *7*, 1566–1572.
- [51] W. Alsalahi and A. M. Trzeciak, *RSC Adv.* **2014**, *4*, 30384–30391.
- [52] W. Alsalahi and A.M. Trzeciak, *J. M. Catal. A: Chem.* **2015**, *408*, 147–151.
- [53] W. Alsalahi, A.M. Trzeciak, *J. Mol. Catal. A: Chem.* **2016**, *423*, 41–48.
- [54] Y. S. Varshavsky and T. G. Cherkasova, *Zh. Neorg. Khim.* **1967**, *12*, 1709.
- [55] G. A. Rempel, P. Legzdins, H. Smith, G. Wilkinson and D. A. Ucko, *Inorg. Synth.*, **1972**, *13*, 90–91.
- [56] A. Sánchez, M. Fang, A. Ahmed and R. A. Sánchez-Delgado, *Appl. Catal., A, General* **2014**, *477*, 117–124.
- [57] Q. Yao, Z. H. Lu, Y. Jia, X. Chen and Xin Liu, *Int. J. Hydrogen Energy* **2015**, *40*, 2207–2215.
- [58] Z. Weng-Sieh, R. Gronsky, and A. T. Bell, *J. Catal.* **1997**, *170*, 62–74.
- [59] S. Suhonen, M. Valden, M. Hietikko, R. Laitinen, A. Savimäki and M. Harkonen, *Appl. Catal. A: Gen.* **2001**, *218*, 151–160.
- [60] D. Ozhava and S. Ozkar, *Int. J. hydrogen energy* **2015**, *40*, 10491–10501.
- [61] J. F. Munera, S. Irusta, L. M. Cornaglia, E. A. Lombardo, D. V. Cesar and M. Schmal, *J. Catal.* **2007**, *245*, 25–34.
- [62] T. L. Barr, *J. Phys. Chem.* **1978**, *82*, 1801–1810.
- [63] A. A. Tolia, R. J. Smiley, W. N. Delgass, C. G. Takoudis and M. J. Weaver, *J. Catal.* **1994**, *150*, 56–70.

- [64] A. Vityuk, H. A. Aleksandrov, G. N. Vayssilov, S. Ma, O. S. Alexeev, and M. D. Amiridis, *J. Phys. Chem. C* **2014**, *118*, 26772–26788.
- [65] J. Wrzyszczyk, M. Zawadzki, A. M. Trzeciak, W. Tylus, and J. J. Ziółkowski, *Catal. Lett.* **2004**, *93*, 85–92.
- [66] Y. V. Larichev, O. V. Netskina, O. V. Komova and V. I. Simagina, *Int. J. hydrogen energy* **2010**, *35*, 6501–6507.
- [67] H. J. Gysling, J. R. Monnier, G. Apai, *J. Catal.* **1987**, *103*, 407–418.
- [68] Y. Okamoto, N. Ishida, T. Imanaka and S. Teranishi, *J. Catal.* **1979**, *58*, 82–94.
- [69] A. M. Trzeciak, M. Jon and J. J. Ziółkowski, *React. Kinet. Catal. Lett.*, **1982**, *20*, 383–387.